



# Localized solar heating via graphene oxide nanofluid for direct steam generation

Mohammad Mustafa Ghafurian<sup>1</sup> · Hamid Niazmand<sup>1,4</sup> · Ehsan Ebrahimnia-Bajestan<sup>2,3</sup> · Hamed Elhami Nik<sup>1</sup>

Received: 31 May 2018 / Accepted: 21 June 2018 / Published online: 5 July 2018  
© Akadémiai Kiadó, Budapest, Hungary 2018

## Abstract

In the present paper, the performance of the graphene oxide in the solar steam generation has experimentally been examined. For this purpose, a setup was built for measuring the evaporation rate, which consists of a solar simulator with a xenon lamp as a radiation source, a pyranometer for light intensity measuring, and a sensory system for measuring the temperature and the mass. Then, the nanofluid with three nanoparticle mass concentrations of 0.001, 0.002, and 0.004% was prepared and exposed to the light intensity of 3.5 Suns ( $3.5 \text{ kW m}^{-2}$ ). Finally, the effects of the light intensity variations on the solar steam generation were studied at the steady and transition conditions. The results showed that the examined carbon nanostructure is efficiently capable of direct solar energy harvesting, such that a maximum total efficiency of 78.9% at 3.5 Suns can be obtained, while the corresponding value for the case of pure water is about 54%. Furthermore, it was found that increasing the light intensity from 1.5 to 3.5 Suns enhances the evaporation flux rate, yet, reduces the evaporation efficiency.

**Keywords** Solar steam generation · Nanofluid · Graphene oxide · Solar simulator

## List of symbols

$A$	Surface area ( $\text{m}^2$ )
Abs	Light absorption (a.u.)
$C_p$	Specific heat capacity ( $\text{kJ kg}^{-1} \text{K}^{-1}$ )
$h_{fg}$	Enthalpy of phase change ( $\text{kJ kg}^{-1}$ )
$I$	Light intensity ( $\text{kW m}^{-2}$ )
$M$	The initial mass of working fluid (g)
$\dot{m}$	Water evaporation flux rate ( $\text{kg m}^{-2} \text{h}^{-1}$ )
$T$	Temperature ( $^{\circ}\text{C}$ )
$t$	Time (s)

## Greek symbols

$\eta$	Efficiency (%)
$w$	Nanoparticle mass fraction (%)

## Index

amb Ambient

## Introduction

Along with the population growth, energy demand has always been an important and strategic issue in economy and industry [1]. Solar energy has been considered as an abundant, renewable, and clean alternative energy to eliminate the undesired consequences of fossil fuels and nuclear energy. One of the well-known methods of solar energy harvesting is absorbing the sunlight by water for the steam generation [2, 3]. However, the low efficiency of these energy conversion systems is still one of the major obstacles to their commercialization. Basically, a large amount of energy is lost in the traditional solar energy harvesting systems. In the traditional solar energy harvesting systems, the solar radiation is absorbed and converted into heat by a surface absorber, and then the thermal energy is transferred to the fluid. Therefore, the absorber temperature may be significantly higher than the ambient temperature, leading to the high radiative and convective losses.

✉ Hamid Niazmand  
niazmand@um.ac.ir

<sup>1</sup> Department of Mechanical Engineering, Ferdowsi University of Mashhad, Mashhad, Iran

<sup>2</sup> Department of Mechanical Engineering, Quchan University of Technology, Quchan, Iran

<sup>3</sup> BioMEMS and Bioinspired Microfluidic Laboratory, Department of Mechanical and Manufacturing Engineering, University of Calgary, Calgary, AB T2N 1N4, Canada

<sup>4</sup> P.O.B. 9177948944, Mashhad, Iran

Therefore, the researchers are looking for a way to reduce the energy losses and increase the solar energy harvesting efficiency, which leads to proposing some innovative methods [3, 4]. A recent promising medium for solar steam generation is nanofluid, which has shown a great ability to absorb the light, and convert it to heat. Nanofluids directly absorb the solar radiation and locally increase the fluid temperature, without significantly increasing the bulk temperature, which in turn reduces the heat loss to the ambient and increases the evaporation efficiency.

As the early studies in this field, one can refer to the solar steam generation using a dispersion of gold nanoparticles into water [5, 6]. The results showed that the amount of energy equal to 1.4 times the energy of the sunlight can generate direct steam from the gold nanofluid with the efficiency of 24%. Following the pioneering work of the Neumann [5, 6], many similar studies were carried out such as Ni et al. [7], Li et al. [8], Jin et al. [9], Wang et al. [10], Amjad et al. [11], Fu et al. [12], Wang et al. [13], Shi et al. [14], Wang et al. [15], Liu et al. [16], and Wang et al. [17]. In these studies, various nanoparticles types were dispersed into water to generate steam by light, including carbon black and graphene nanoparticles [7], graphene and graphene–Au nanocomposite [12], Ag@TiO<sub>2</sub> [8], gold [9, 11, 13], single and multi-wall carbon nanotube functionalized with carboxyl group [10, 14, 17], Ti<sub>2</sub>O<sub>3</sub> [15], reduced graphene oxide [16]. Consequently, the total efficiencies of 80.3% [9], 95% [11] and 59.2% [12] at the intensities of 220, 280, and 16.77 Suns, respectively, were reported in the case of the gold nanoparticle. However, the evaporation efficiencies of 46.8% [10], 60.3% [14], 60% [7] 66.9% [8] and 48% [17] were obtained from other nanoparticles at intensities higher than 10 Suns.

Surveying the literature shows that the solar steam generation using nanofluids is a novel topic still with many gaps that should be covered. For instance, finding efficient, yet cost-effective nanoparticles and the performance of the nanofluids at low sunlight intensities need more investigations. Therefore, the purpose of this study is to experimentally examine the solar energy harvesting using graphene oxide (GO) nanoparticles dispersed into water. The reasons for choosing graphene oxide are: (1) the unique shape and characteristics of this nanoparticle compared to others; (2) the promising ability of the carbon nanostructures in light absorption; (3) the expected proper stability of this nanoparticle into water due to the oxygen functional groups attached to GO.

To investigate the performance of this nanofluid in the solar steam generation, a solar simulator has been employed. Then, the effects of different parameters such as nanoparticle concentration and light intensity on the fluid

temperature, evaporation flux rate, and efficiency have been examined in detail. The performance of the prepared nanofluid in relatively lower light intensities has also been studied, for the first time.

## Experimental

### Nanofluid preparation

A water-based nanofluid containing GO nanoparticles with thickness of 1–10 nm was studied at three mass fractions (0.001, 0.002, and 0.004%) purchased from Vira Carbon Nano Materials Co, where a two-step method had been used to prepare the nanofluids. Figure 1a shows the TEM image of these nanoparticles after dispersing into water.

Figure 1b exhibits the prepared nanofluids at different GO mass fractions. To examine the stability, the zeta potential of the nanofluid was measured by ZetaCompact device, which showed the value of  $-32.21$  mV at actual pH of 6. In general, a nanofluid with the absolute value of zeta potential  $> 30$  mV is considered relatively stable [18, 19]. Also, visual inspection confirmed the appropriate stability of all samples during the evaporation tests ( $< 10$  h).

### Solar steam generation setup

Figure 2 shows the setup designed for solar steam generation. The main components are a solar simulator (a 1600-W xenon lamp with the radiation temperature of 6000 K), a glass container (a beaker with the height of 70 mm and the diameter of 38 mm) containing working fluid, temperature sensors, a digital weighting scale (kernel with a precision of 0.0001, Germany), CMP3 secondary standard pyranometer (purchased from Kipp & Zonen Co. with the precision of  $1 \text{ W m}^{-2}$  in the wavelength of 200–2800 nm interval), and a designed and built data logger system. Three sensors are located at 10, 30, and 50 mm from the bottom of the beaker to measure the time variations of the fluid temperature at different depths. The

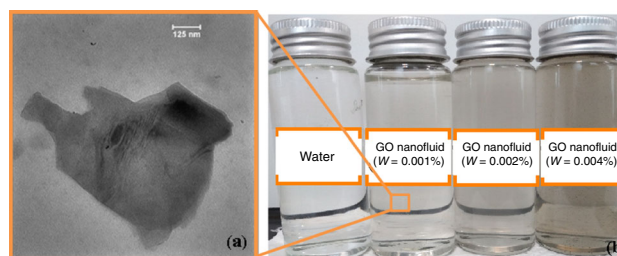


**Fig. 1** a TEM image of graphene oxide (GO) dispersed into water; b GO/water nanofluid samples at different concentrations compared to water

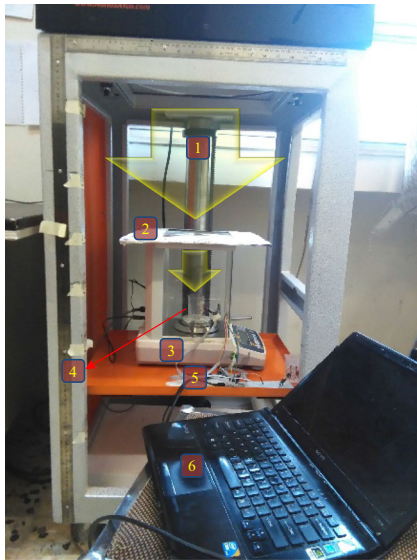


**Fig. 2** Solar simulator and steam generation setup; (1) path of light generated by solar simulator (2) Fresnel lens, (3) digital weighting scale, (4) beaker and sensors, (5) data logger, and (6) a PC system for collecting data during the test

upper side of all sensors, which is exposed to the radiation, is covered with a silicon adhesive to prevent the radiation effects on the measuring process. All sensors are PT100 type (Class AA), which were calibrated by Meyar Saze Bartar Researching Institute at different temperatures (5, 10, 20, 30, 40, 50, 80, and 100 °C). The calculated uncertainties in temperature measurement due to the repeatability and equipment accuracy are 0.4 and 0.01 °C, respectively, which leads to the total uncertainty of 0.40 °C.

In every test, the beaker is filled with 60 mL water or nanofluid; the solar simulator is turned on, and the required light intensity is obtained by adjusting the distance between the xenon lamp and the sample according to the type of Fresnel lens. The pyranometer ensures us about having the desired light intensity. The evaporated water is measured during the test by weighting the remained liquid, which is recorded by a computer. The fluid temperature at three different elevations, besides the ambient temperature, is measured and recorded.

## Results and discussion

One of the significant properties of a fluid in terms of solar heating and evaporation is the ability to absorb light. Therefore, the ability of the samples to absorb the visible light was examined by a spectrophotometric apparatus (Agilent 8453 Model), with the optical pass length of 10 mm, and water as the reference medium. Figure 3

depicts the absorption spectra of different nanofluid samples (Fig. 3a) as compared to the pure water (Fig. 3b) in the wavelength range of 300–800 nm, which covers the visible wavelength, as done in some available studies [10, 12, 19]. Figure 3b indicates the relative weak sunlight absorption of water. Adding nanoparticles to water leads to a significant increase in the visible light absorption. It can be seen that the GO nanofluid can increase the visible light absorption of pure water by about 23 times at a very low GO mass fraction of 0.004%. Additionally, higher nanoparticle concentration is associated with the larger amount of light absorption.

To examine the evaporation performance, the nanofluids inside the beaker were exposed to the light generated by the solar simulator. Figures 4 and 5 display the fluid temperature rise ( $T_1$ ,  $T_2$ , and  $T_3$ ) and ambient temperature rise ( $T_{amb}$ ) at the light intensity of 3.5 Suns (1 sun = 1 kW m<sup>-2</sup>), for pure water and the nanofluid of 0.004 mass%, respectively. The temperature rise is the temperature difference between the real time temperature during light exposure and the initial temperature of the fluid or air at the start of the test. In these figures,  $T_1$  denotes the fluid temperature at the highest level (50 mm above the beaker base), while  $T_3$  is the deepest level (which is 10 mm above the beaker base), and  $T_{amb}$  is the

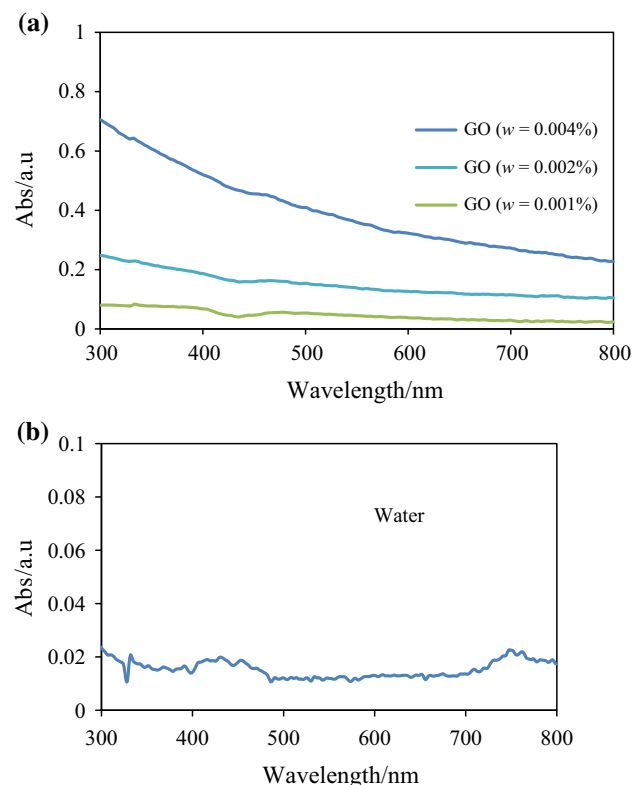


**Fig. 3** Absorption spectra for **a** the GO nanofluids at various concentrations, and **b** water

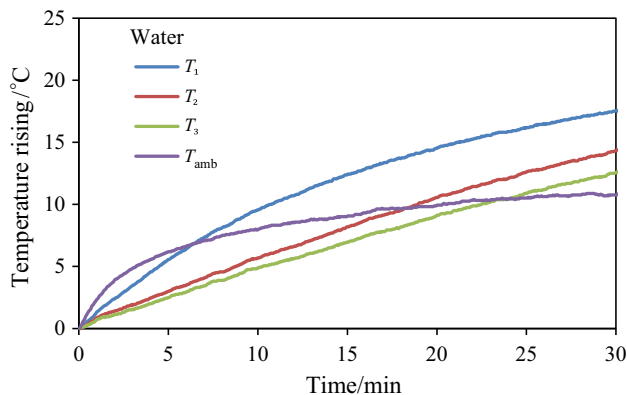


**Fig. 4** The temperature rise of water and the ambient temperature at the light intensity of 3.5 Suns

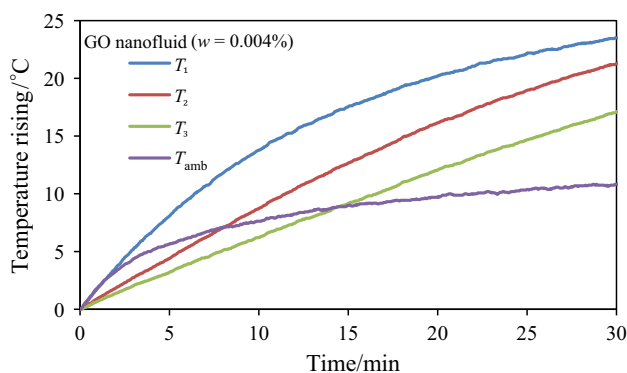


**Fig. 5** The temperature rise of the GO nanofluids at 0.004 mass% concentration and the ambient temperature at the light intensity of 3.5 Suns

ambient temperature close to the beaker. As it can be seen, after 30 min of light exposure,  $T_1$  shows about 23.5 °C increase for the nanofluid, while this temperature rise is about 17 °C for the pure water. Note that the ambient temperature rise is almost identical for both cases. The observed increase in the temperature of the nanofluid indicates the proper performance of GO nanoparticles in light energy absorption and heat loss reduction.

On the other hand, Figs. 4 and 5 show that the temperature in the surface region of the working fluids increases more than that of the lower layers, which indicates that the light absorption is more pronounced at the upper layers of the fluid. This can be explained by the Beer–Lambert law [22], which states that the major portion of the light passed through a colloid is absorbed in the first exposed layers.

The effect of the nanoparticle concentration on the solar evaporation is illustrated in Figs. 6 and 7, showing the time variations of temperature rise in the upper layers of the working fluids, and the mass of evaporated water, respectively. It can be concluded that increasing the nanoparticle

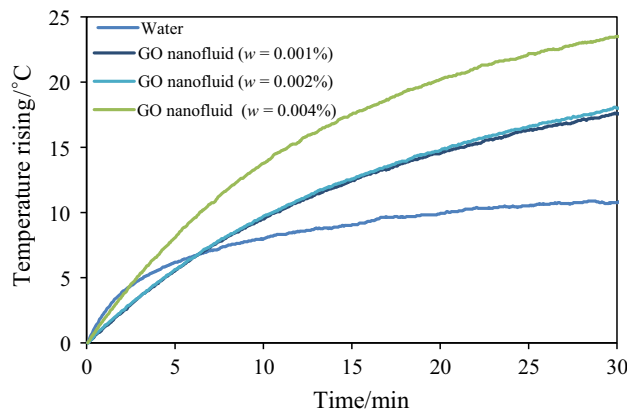


**Fig. 6** Temperature rise registered by sensor  $T_1$  for GO nanofluid at different nanoparticles concentrations compared to that of water, at the light intensity of 3.5 Suns

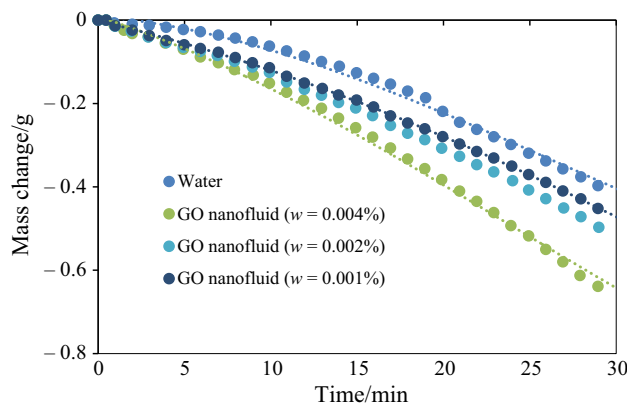


**Fig. 7** Time variations of the reduced mass of the GO nanofluid at different nanoparticle concentrations compared to that of water exposed to the light intensity of 3.5 Suns

concentration enhances the evaporation flux rate, which confirms the results of the absorption spectra in Fig. 3, and is also consistent with the findings of other researchers [10, 20, 21]. The highest evaporation flux rate related to the nanofluid with the highest GO concentration is about  $1.25 \text{ kg m}^{-2} \text{ h}^{-1}$ , which is 1.6 times more than that of water.

Up to this stage, all tests were carried out at the intensity of 3.5 Suns. In this section, the effect of light intensity is examined on the evaporation flux rate at GO concentration of 0.004 mass%. It should be mentioned that the light intensity alters by adjusting the distance of the radiation source to the samples and changing the type of Fresnel lens. Figures 8 and 9 show the temperature rise registered by  $T_1$  sensor and the amount of evaporated mass, respectively, during the 30-min test run. Based on the results, as the light intensity increases from 1.5 to 3.5 Suns, the temperature of the upper layers of the nanofluid significantly rises, and the amount of evaporated mass after

30 min increases by 50% as compared to that of pure water.

For evaluating the performance of solar energy harvesting, the evaporation, sensible heating, and total photo-thermal efficiencies are presented in this section. Evaporation efficiency is defined as the ratio of the latent energy of evaporation in the steam production process to the total input light to the fluid [7, 9, 12]:

$$\eta_{\text{evaporation}} = \frac{\dot{m}h_{\text{fg}}}{I} \tag{1}$$

where  $\dot{m}(\text{kg h}^{-1} \text{m}^{-2}) = \Delta m/(At)$  is the water evaporation flux rate,  $A (\text{m}^2)$  is the effective surface of fluid exposed to the light,  $t (\text{h})$  is the illumination time,  $h_{\text{fg}}$  is the enthalpy of phase change ( $2357 \text{ kJ kg}^{-1}$  at 1 atmosphere pressure for water), and  $I (\text{W m}^{-2})$  is the input light intensity. Note that similar to available researches [7, 9, 12, 20, 21], the latent heat of evaporation for nanofluid is assumed to be the same as that of water. In addition, sensible heating efficiency is defined as the amount of

consumed heat for the fluid heat up divided by the total input radiation as follows [7, 9, 12]:

$$\eta_{\text{sensible heating}} = \frac{M \times C_p \times \Delta T/t}{I \times A} \tag{2}$$

where  $M (\text{kg})$  is the initial mass of working fluid,  $C_p (\text{kJ kg}^{-1} \text{K}^{-1})$  is the specific heat capacity of the fluid, and  $\Delta T$  is the fluid temperature rise during the time  $t$ . In this calculation, the fluid temperature is the average of the temperature values recorded by three sensors inside the fluid. For  $C_p$ , the amount of specific heat capacity of water at one bar pressure is used for all cases, due to the very low concentrations of nanoparticles in the studied nanofluid. Finally, total photo-thermal efficiency [16, 17, 23] is calculated as Eq. (3).

$$\eta_{\text{total}} = \eta_{\text{evaporation}} + \eta_{\text{sensible heating}} \tag{3}$$

Figures 10 and 11 present the calculated efficiencies for water and 0.004 mass% GO nanofluid, respectively, at different light intensities. According to these figures, adding nanoparticle leads to the enhancements of evaporation, sensible heating, and total efficiencies, respectively, by 10, 16, and 26% as compared to those of water. An interesting finding is that the highest evaporation efficiency occurs at the lowest intensity of 1.5 Suns. This finding was also observed by other researchers [8, 14, 24]. Increasing the light intensity leads to the increase in temperature of nanoparticles and the fluid around the particles, which is desirable for heat localizing and steam generation. However, at higher light intensities, the portion of the absorbed energy used for the fluid heat up increases due to the deeper penetration of the light into the fluid, which is evident by considering the sensible heating efficiencies, which increase with the increase in light intensity. The competition between these two opposite phenomena determines the efficiency of evaporation. As shown in Fig. 11, the total efficiency of photo-thermal energy conversion is nearly constant for the examined light intensities, while the sensible heat efficiency increases by light intensification.

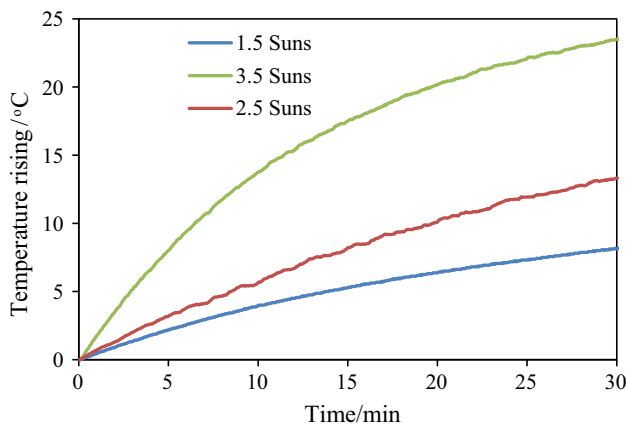


Fig. 8 Time variations of temperature rise registered by  $T_1$  sensor for 0.004 mass% GO nanofluids at different light intensities

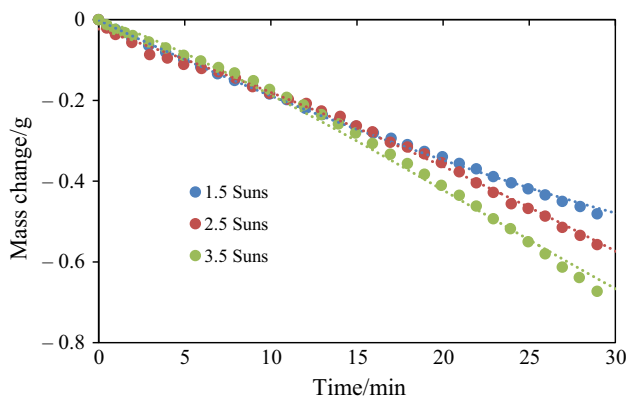


Fig. 9 Time variations of the fluid mass reduction for 0.004 mass% GO nanofluids at different light intensities

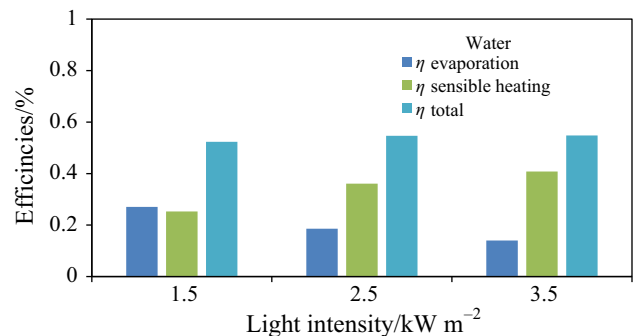
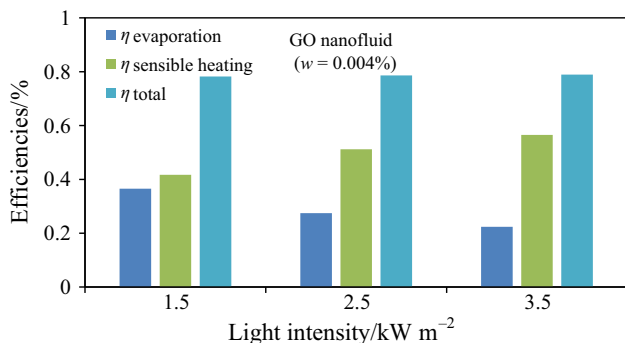


Fig. 10 The sensible heating, evaporation, and total efficiencies of pure water at different light intensities





**Fig. 11** The sensible heating, evaporation, and total efficiencies of 0.004 mass% GO nanofluid at different light intensities

Finally, to compare the performance of the GO nanofluid in the solar steam generation with other nanofluids examined in previous studies, Fig. 12 is presented. Different nanoparticle types have been studied for enhancing the solar steam generation. Generally, the aim of this technique is localizing the light absorption and photo-thermal energy conversion. In this regard, the materials with strong ability of light absorption such as carbon nanomaterials have been used. Also, the plasmonic nanoparticles such as gold, which can convert the electromagnetic radiation to the heat, due to the special band gap between conductance and valance bands, are proper candidates for localizing the solar heating.

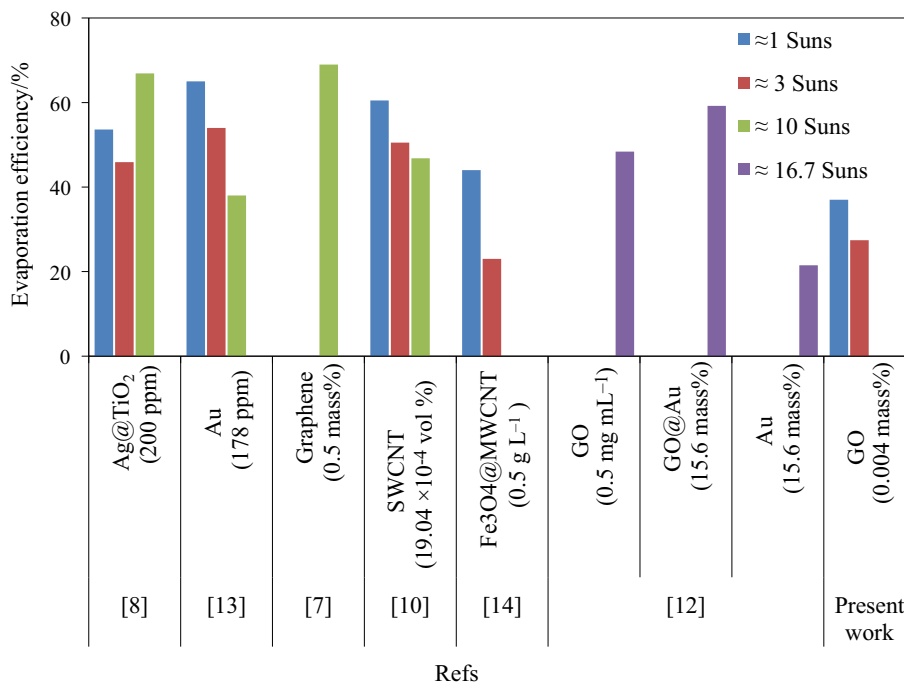
Considering Fig. 12, the researches indicate the significant performance of the composite nanoparticles, such as Ag@TiO<sub>2</sub>, Fe<sub>3</sub>O<sub>4</sub>@MWCNT, and also gold nanoparticles in the solar steam generation. However, the complicated

processes of synthesizing the nanocomposite materials and graphene in addition to the high cost of the required chemicals for Au nanoparticle synthesis make these nanomaterials very expensive as compared to the GO nanoparticles. Furthermore, the stability of the GO nanoparticles in water is basically higher than other nanoparticles listed in Fig. 12, due to the oxygen functional groups attached to GO. The evaporation efficiency of the studied GO nanofluid is also comparable with the other nanofluids. Consequently, the graphene oxide nanofluid can be considered as a reasonable candidate for enhancing the efficiency of solar steam generation, at relatively lower light intensities.

### Conclusions

In this study, the performance of graphene oxide nanoparticles in the solar steam generation was examined in detail, employing a solar simulator setup. The effects of nanoparticle concentration (0.001, 0.002, and 0.004 mass%) and light intensity (1.5, 2.3, and 3.5 Suns) were investigated on the visible light absorption, fluid temperature rise, evaporation flux rate, and efficiency. The results demonstrated the proper capability of this nanofluid in direct solar energy absorption and steam production. An evaporation efficiency of 36.54% was achieved by this nanofluid at the low light intensity of 1.5 Suns and low nanoparticle concentration of 0.004 mass%. The cost-effective synthesis and proper stability of GO nanofluid are

**Fig. 12** Comparison of the reported evaporation efficiencies for different nanofluids and light intensities



the other considerable advantages of this nanoparticle, which are very important in terms of commercialization.

## References

- Ghafurian MM, Niazmand H. New approach for estimating the cooling capacity of the absorption and compression chillers in a trigeneration system. *Int J Refrig*. 2018;86:89–106.
- Chang C, Yang C, Liu Y, Tao P, Song C, Shang W, Wu J, Deng T. Efficient solar-thermal energy harvest driven by interfacial plasmonic heating-assisted evaporation. *ACS Appl Mater Interface*. 2016;8:23412–8.
- Mahian O, Kianifar A, Zeinali Heris A, Wen D, Sahine AZ, Wongwises S. Nanofluids effects on the evaporation rate in a solar still equipped with a heat exchanger. *Nano Energy*. 2017;36:134–55.
- Hjerrild NE, Taylor RA. Boosting solar energy conversion with nanofluids. *Phys Today*. 2017;70(12):40–5.
- Neumann O, Urban AS, Day J, Lal S, Nordlander P, Halas NJ. Solar vapor generation enabled by nanoparticles. *ACS Nano*. 2013;7:42–9.
- Neumann O, Feronti C, Neumann AD, Dong A, Schell K, Lu B, et al. Compact solar autoclave based on steam generation using broadband light-harvesting nanoparticles. *Proc Natl Acad Sci*. 2013;110:11677–81.
- Ni G, Miljkovic N, Ghasemi H, Huang X, Boriskina SV, Lin C-T, et al. Volumetric solar heating of nanofluids for direct vapor generation. *Nano Energy*. 2015;17:290–301.
- Li H, He Y, Liu Z, Huang Y, Jiang B. Synchronous steam generation and heat collection in a broadband Ag@TiO<sub>2</sub> core-shell nanoparticle-based receiver. *Appl Therm Eng*. 2017;121:617–27.
- Jin H, Lin G, Bai L, Zeiny A, Wen D. Steam generation in a nanoparticle-based solar receiver. *Nano Energy*. 2016;28:397–406.
- Wang X, He Y, Cheng G, Shi L, Liu X, Zhu J. Direct vapor generation through localized solar heating via carbon nanotube nanofluid. *Energy Convers Manag*. 2016;130:176–83.
- Amjad M, Raza Gh, Xin Y, Pervaiz Sh, Xu Ji DuX, Wen D. Volumetric solar heating and steam generation via gold nanofluids. *Appl Energy*. 2017;206:393–400.
- Fu Y, Mei T, Wang G, Guo A, Dai G, Wang Sh, Wang J, Li J, Wang X. Investigation on enhancing effects of Au nanoparticles on solar steam generation in graphene oxide nanofluids. *Appl Therm Eng*. 2017;114:961–8.
- Wang X, He Y, Liu X, Shi L, Zhu J. Investigation of photothermal heating enabled by plasmonic nanofluids for direct solar steam generation. *Sol Energy*. 2017;157:35–46.
- Shi L, He Y, Huang Y, Jiang B. Recyclable Fe<sub>3</sub>O<sub>4</sub>@CNT nanoparticles for high-efficiency solar vapor generation. *Energy Convers Manag*. 2017;149:401–8.
- Wang J, Li Y, Deng L, Wei N, Weng Y, Dong S, Qi D, Qiu J, Chen X, Wu T. High-performance photo thermal conversion of narrow-bandgap Ti<sub>2</sub>O<sub>3</sub> nanoparticles. *Adv Mater*. 2017;29:1603730.
- Liu X, Wang X, Huang J, Cheng G, He Y. Volumetric solar steam generation enhanced by reduced graphene oxide nanofluid. *Appl Energy*. 2018;220:302–12.
- Wang X, He Y, Liu X, Zhu J. Enhanced direct steam generation via a bio-inspired solar heating, method using carbon nanotube films. *Powder Technol*. 2017;321:276–85.
- Ghadimi A, Saidur R, Metselaar HSC. A review of nanofluid stability properties and characterization in stationary conditions. *Int J Heat Mass Transf*. 2011;54:4051–68.
- Ahmed Sharafeldina M, Gróf G, Mahian O. Experimental study on the performance of a flat-plate collector using WO<sub>3</sub>/water nanofluids. *Energy*. 2017;141:2436–44.
- Ghafurian MM, Niazmand H, Ebrahimnia bejestan E. Performance evaluation of multi-wall carbon nanotube in solar fresh water production. *Articles in Press, Amirkabir Journal of Mechanical Engineering, Accepted Manuscript, Available Online from 12 May 2018*.
- Zielinski MS, Choi JW, La Grange T, Modestino M, Hashemi SM, Pu Y, Birkhold S, Hubbell JA, Psaltis D. Hollow mesoporous plasmonic nanoshells for enhanced solar vapor generation. *Nano Lett*. 2016;13:2159–67.
- Swinehar DF. The Beer–Lambert law. *J Chem Educ*. 1962;39:333.
- Wang X, He Y, Liu X, Cheng G, Zhu J. Solar steam generation through bio-inspired interface heating of broadband-absorbing plasmonic membranes. *Appl Energy*. 2017;195:414–25.
- Ghasemi H, Ni G, Marconnet AM, Loomis J, Yerci S, Miljkovic N, et al. Solar steam generation by heat localization. *Nat Commun*. 2014;5:4449.